MICROBIOLOGY

RESEARCH ARTICLE

Switzer *et al.*, *Microbiology* 2018;164:1457–1470

DOI 10.1099/mic.0.000683

MICROBIOLOGY SOCIETY

OPEN MICROBIOLOGY

EDITOR'S CHOICE

A novel regulatory factor affecting the transcription of methionine biosynthesis genes in *Escherichia coli* experiencing sustained nitrogen starvation

Amy Switzer,[1] Dimitrios Evangelopoulos,[2] Rita Figueira,[1] Luiz Pedro S. de Carvalho,[2] Daniel R. Brown[1,*] and Sivaramesh Wigneshweraraj[1,*]

Abstract

The initial adaptive transcriptional response to nitrogen (N) starvation in *Escherichia coli* involves large-scale alterations to the transcriptome mediated by the transcriptional activator, NtrC. One of these NtrC-activated genes is *yeaG*, which encodes a conserved bacterial kinase. Although it is known that YeaG is required for optimal survival under sustained N starvation, the molecular basis by which YeaG benefits N starved *E. coli* remains elusive. By combining transcriptomics with targeted metabolomics analyses, we demonstrate that the methionine biosynthesis pathway becomes transcriptionally dysregulated in Δ*yeaG* bacteria experiencing sustained N starvation. It appears the ability of MetJ, the master transcriptional repressor of methionine biosynthesis genes, to effectively repress transcription of genes under its control is compromised in Δ*yeaG* bacteria under sustained N starvation, resulting in transcriptional derepression of MetJ-regulated genes. Although the aberrant biosynthesis does not appear to be a contributing factor for the compromised viability of Δ*yeaG* bacteria experiencing sustained N starvation, this study identifies YeaG as a novel regulatory factor in *E. coli* affecting the transcription of methionine biosynthesis genes under sustained N starvation.

INTRODUCTION

Conditions that sustain constant bacterial growth are seldom found in nature. Environments where growth is limited by availability of nutrients are common, for example, soil, water, or even host environments such as macrophages can lack essential nutrients to support growth. As such, many bacteria spend most of their time in states of little or no growth due to starvation. The starved and growth attenuated state is now widely considered as an important physiological condition in bacterial pathogenesis and survival. Nitrogen (N) is an essential element of most macromolecules (proteins, nucleic acids and cell wall components) within a bacterial cell. Many bacterial pathogens appear to experience N limitation in host environments such as the urinary tract (e.g. uropathogenic *Escherichia coli* [1]) or macrophages (e.g. *Salmonella* Typhimurium [2]), and respond by activating specific adaptive processes. Emerging evidence also indicates that bacterial N metabolism and N stress responses have a role in the development of dysbiosis [3]. Further, we recently reported that the specific adaptive response to N starvation in *E. coli* is directly coupled to the production of guanosine pentaphosphate, (p)ppGpp: the pleiotropic stress signalling nucleotide and effector of the stringent response [4, 5]. Thus, the adaptive response to N starvation clearly plays an integral and fundamental role in bacterial physiology and pathogenesis.

The initial adaptive response to N starvation is mediated by the transcriptional activator, NtrC, and involves the expression of genes largely associated with activation of transport systems, catabolic and biosynthetic operons for the scavenging of alternative N sources, transcriptional reprogramming and managing cellular resources until growth conditions

Received 18 April 2018; Accepted 2 June 2018

Author affiliations: [1]MRC Centre for Molecular Bacteriology and Infection, Imperial College London, London, SW7 2AZ, UK; [2]Mycobacterial Metabolism and Antibiotic Research Laboratory, The Francis Crick Institute, 1 Midland Road, London, NW1 1AT, UK.

***Correspondence:** Daniel R. Brown, d.brown06@imperial.ac.uk; Sivaramesh Wigneshweraraj, s.r.wig@imperial.ac.uk

Keywords: *Escherichia coli*; nitrogen starvation; transcription regulation; transcription repressor; MetJ; methionine biosynthesis.

Abbreviations: ChIP, chromatin immunoprecipitation; COG, clusters of orthologous groups; LB, Luria–Bertani; LC-MS, liquid chromatography mass spectrometry; N, nitrogen; (p)ppGpp, guanosine pentaphosphate; RNAP, RNA polymerase; RNA-seq, RNA sequencing; SAH, S-adenosylhomocysteine; SAM, S-adenosylmethionine; TA, toxin-antitoxin.

The RNA sequencing data have been deposited in the ArrayExpress database at EMBL-EBI (www.ebi.ac.uk/arrayexpress), under accession number E-MTAB-6481.

Four supplementary tables, six supplementary figures and two supplementary movies are available with the online version of this article.

improve. One of the most highly expressed operons during the initial adaptive response to N starvation consists of *yeaG* and *yeaH*. Both genes are conserved across several bacterial species, especially Enterobacteriaceae, including plant and animal pathogenic bacteria (e.g. *Shigella*, *Salmonella*, *Erwinia* and *Pseudomonas* species) [5–7]. They are also induced in response to diverse stresses (including low pH [8], high osmolarity [9], stationary phase [8] and low sulphur [10]), which suggests a wider importance of *yeaG* and *yeaH* and pathways affected by them in bacterial adaptive processes. Although the product of *yeaH* has no sequence or structural homology to any known protein, YeaG is a Hank's type kinase [11, 12].

In earlier work, we revealed that the viability of Δ*yeaG E. coli* becomes significantly compromised only after 24 h under N starvation and thus proposed a role for YeaG in the adaptive response to sustained N starvation [6]. Further, we showed that the intracellular concentration of RpoS (σ^{38}), the major bacterial sigma (σ) factor required for the transcription of general stress response genes, was decreased by more than twofold in Δ*yeaG* bacteria compared to the wild-type [6], and consequently suggested that Δ*yeaG* bacteria might be compromised to effectively adapt their transcriptional programme to survive a sustained period of time under N starvation. In the present study, we compare the transcriptomes of wild-type and Δ*yeaG* bacteria to assess how YeaG affects the transcriptional response to N starvation. The results reveal that YeaG plays a role in the adaptive response to initial and sustained nitrogen starvation, and identifies YeaG as a novel regulatory factor in *E. coli* affecting the transcription of methionine biosynthesis genes under sustained N starvation.

METHODS

Bacterial strains, plasmids, growth conditions and viability measurements

Strains and plasmids used in this study were derived from *Escherichia coli* K-12 and are listed in Table S1 (available in the online version of this article). The NtrC-FLAG allele was transduced into the BW25113 strains (wild-type and Δ*yeaG*) using P1 phage transduction from the NtrC-FLAG NCM3722 strain as described in [5]. The *metJ*-FLAG strains were constructed using the λ Red recombinase method to introduce an in-frame fusion encoding three repeats of the FLAG epitope [3×(DYKDDDDK)] followed by a kanamycin resistance cassette, amplified from the pDOC-F plasmid [13], to the 3′ end of *metJ*. The Δ*metJ* strain was also constructed using the λ Red recombinase method to introduce an in-frame fusion encoding a kanamycin resistance cassette amplified from the pDOC-K plasmid [13] in place of the *metJ* gene in the wild-type BW25113 strain. Bacteria were grown in Gutnick minimal medium (33.8 mM KH_2PO_4, 77.5 mM K_2HPO_4, 5.74 mM K_2SO_4, 0.41 mM $MgSO_4$), supplemented with Ho-LE trace elements [14] and 0.4 % (w/v) glucose according to Figueira *et al.* [6], where the sole source of nitrogen is NH_4Cl; overnight cultures were grown in medium containing 10 mM NH_4Cl and N-limiting growth curves were carried out in medium containing 3 mM NH_4Cl. To measure the biological activity of MetJ-FLAG, the *metJ*-FLAG strains were grown in Luria–Bertani (LB) medium supplemented with 100 μg ml^{-1} methionine to induce repression of the methionine biosynthesis pathway as described in [15]. Samples were taken during exponential growth for analysis of *metF* transcript levels as described below by quantitative reverse transcription PCR. All growth curves were generated by measuring the optical density ($OD_{600\ nm}$) of the bacterial cultures over time. The number of viable cells was determined by measuring c.f.u. ml^{-1} from serial dilutions on LB agar plates at the designated time points shown in Fig. 1.

Antisera and immunoblotting

Immunoblotting was completed according to standard laboratory protocols [16]. To produce antiserum against YeaG, His-tagged YeaG (expressed from the arabinose-inducible plasmid: pBAD18-*yeaG* in MC1061) was purified using nickel affinity purification. Eurogentec produced the antiserum against YeaG through immunization of rabbits with the purified YeaG protein. This protein was also used to affinity-purify the antibodies from the sera following standard laboratory protocols [16]. The YeaG antibody was used at 1 : 2500 dilution. The following commercial primary antibodies were used: mouse monoclonal anti-RNA polymerase (RNAP) α subunit 4RA2 at 1 : 10 000 dilution (Biolegend), and anti-FLAG M2 at 1 : 1000 dilution (Sigma, F3165). Both secondary antibodies were used at 1 : 10 000 dilution, either rabbit anti-mouse IgG H and L horseradish peroxidase (HRP)-linked secondary antibody (Abcam, ab97046) or Amersham ECL Rabbit IgG, HRP-linked whole antibody (from donkey) (GE Healthcare, NA934). ECL Prime Western blotting detection reagent was used for all the immunoblotting experiments done in this study (GE Healthcare, RPN2232). All blots were analysed on the ChemiDoc MP imaging system and bands quantified using Image Lab software version 5.2.1.

RNA sequencing (RNA-seq)

Cultures were grown as in [6] and sampled at the following time points: N+, when the $OD_{600\ nm}$=0.3; N-, 20 min following N run-out; and N-24, where bacteria were subjected to 24 h of N starvation. Two biological replicates were taken for N+ and N-, and three for N-24. Cultures were mixed with a 1 : 19 phenol:ethanol solution at a ratio of 9 : 1 culture:solution and then pelleted. Cell pellets were sent to Vertis Biotechnologie AG for downstream processing exactly as previously described by [17]. The RNA extracted for RNA-seq was examined by capillary electrophoresis before rRNA depletion, cDNA synthesis and next-generation sequencing. The data analyses were performed with CLC Genomics Workbench 7 using standard parameters. RNA-seq reads were mapped to the *E. coli* K-12 MG1655 (U00096.3) genome using Burrows–Wheeler Aligner. Reads that mapped uniquely were used for further analysis. Total read counts were used to normalize the data, the number of reads

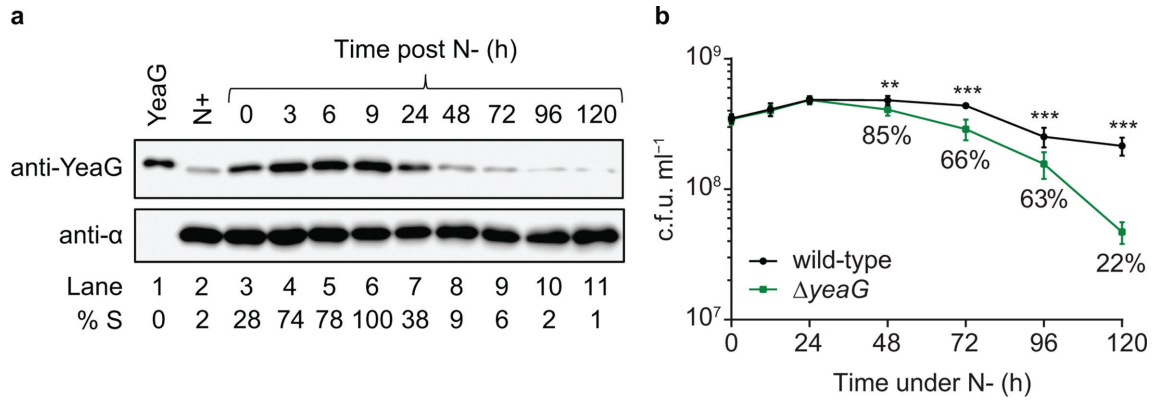

Fig. 1. The initial 24 h of N starvation represents a physiologically important period during which YeaG-mediated adaptation to sustained N starvation occurs. (a) Representative immunoblot of whole-cell extracts of bacterial cells sampled at N+ and after various periods of N starvation probed with anti-YeaG antibody and anti-RNA polymerase α subunit antibody (loading control). Percentage S (% S) indicates the ratio in intensity between the bands corresponding to YeaG and α subunit at each time point. The bands corresponding to YeaG and α subunit shown are from the same blot. (b) Graph showing the viability of wild-type and Δ*yeaG* bacteria as measured by counting c.f.u. over 5 days under sustained N starvation. Values show the percentage of viable bacteria in the Δ*yeaG* mutant compared with the wild-type at each time point. Error bars represent SEM (n=3). Statistical analyses were performed by one-way ANOVA (** P<0.01, ***P<0.001).

mapping to each gene was calculated, and a matrix of read counts was generated. The matrix was analysed using the DESeq2 BioConductor package for differential gene expression analysis. Genes with ≤10 reads mapped to them were excluded from analysis. All statistical analyses were performed in R version 3.4.2. The data have been deposited in the ArrayExpress database at EMBL-EBI (www.ebi.ac.uk/arrayexpress) under accession number E-MTAB-6481.

Quantitative reverse transcription PCR (qRT-PCR)

RNA was acquired and stabilized at specified time points using Qiagen RNA Protect reagent (Qiagen, 76526). RNA extraction was carried out using the PureLink RNA mini kit (Invitrogen, 12183025) and DNase Set (Invitrogen, 12185010). The A260/280 and A260/230 ratios of the extracted RNA for qRT-PCR was analysed and deemed suitable for downstream processing. The High-Capacity cDNA Reverse Transcription kit (Applied Biosystems, 4368814) was used to convert 100 ng of purified RNA to cDNA. 400 ng μl^{-1} of cDNA was used per qRT-PCR reaction containing: 10 µl PowerUp SYBR Green Master Mix (Applied Biosystems, A25742), 1 µl forward primer (5 µM), 1 µl reverse primer (5 µM) and 1 µl template cDNA in a 20 µl reaction volume. Amplifications were performed on the StepOnePlus Real-Time PCR system (Applied Biosystems, 4376600) using the following cycle: 95 °C (10 min) followed by 40 cycles of 95 °C (15 s), 59 °C (15 s), 68 °C (45 s), and a melt curve of 95 °C (15 s), 60 °C (1 min), 95 °C (15 s). Sequences of all primers used in this study are listed in Table S2. All real-time analysis was performed in triplicate and compared against 16S rRNA expression as an internal control.

Metabolomics

Metabolite analysis was carried out using liquid chromatography mass spectrometry (LC-MS)-based metabolomics. Briefly, cultures of wild-type and Δ*yeaG* strains were grown in 100 ml of Gutnick minimal medium in triplicate as described above for the RNA-seq experiment. The cultures were then spun down rapidly at 3000 ***g*** for 5 min, the excess of the supernatant was discarded, and the remaining 10 ml of culture was passed through a 0.22 µm pore size filter (mixed cellulose ester membrane; Millipore #GSWP02500). The metabolites were quenched by submerging the filter containing the bacteria directly into 1 ml solution of acetonitrile: methanol: water (ACN : MeOH : H_2O; 2 : 2 : 1 v/v/v) that was pre-chilled at −40 °C on dry ice. The whole mixture was transferred into a 2 ml screw cap polypropylene tube containing around 400 µl of acid-washed beads (150–212 µm; Sigma #G1145) and ribolysed for 40 s at 6.5 speed. Following lysis, the tubes were centrifuged at 12 000 r.p.m. for 10 min and supernatants containing soluble metabolites were passed into a Spin-X 0.22 µm cellulose acetate centrifuge tube filter (Costar; #8160) and stored at −80 °C. Prior to LC-MS, metabolite samples were mixed with acidified ACN (0.2 % acetic acid) at a 1 : 1 ratio, spun down at top speed for 5 min and transferred into LC-MS vials. LC-MS was performed in an Agilent 1200 LC system coupled with an Agilent Accurate Mass 6230 TOF apparatus using the method as described in [18]. Briefly, the LC system was equipped with a solvent degasser, a binary pump, temperature-controlled auto-sampler and temperature-controlled column compartment with a Cogent Diamond Hydride Type C silica column (150×2.1 mm; dead volume 315 µl) that was employed for liquid chromatography. The

mobile phase method used consisted of 0 min 85 % B; 0–2 min 85 % B; 2–3 min to 80 % B; 3–5 min 80 % B; 5–6 min to 75 % B; 6–7 min 75 % B; 7–8 min to 70 % B; 8–9 min 70 % B; 9–10 min to 50 % B; 10–11 min 50 % B; 11–11.1 min to 20 % B; 11.1–14 min hold 20 % B, where solvent A consists of deionized water with 0.2 % acetic acid and solvent B consists in acetonitrile with 0.2 % acetic acid. The flow rate on Agilent 1200 LC was 0.4 ml min^{-1}. On the Agilent Accurate Mass 6230 TOF apparatus, dynamic mass axis calibration was achieved by continuous infusion of a reference mass solution using an isocratic pump connected to a multimode ionization source, operated in the positive-ion and negative-ion mode. ESI capillary and fragmentor voltages were set at 3500 and 100 V, respectively. The nebulizer pressure was set at 40 p.s.i. and the nitrogen drying gas flow rate was set at 10 l min^{-1}. The drying gas temperature was maintained at 250 °C. The MS acquisition rate was 1.5 spectra s^{-1} and m/z data ranging from 50 to 1200 were stored. This instrument routinely enabled accurate mass spectral measurements with an error of less than 5 parts-per-million (p.p.m.), mass resolution ranging from 10 000 to 25 000 over the m/z range of 121–955 atomic mass units, and a 100 000-fold dynamic range with picomolar sensitivity. Data were collected in the centroid mode in the 4 GHz (extended dynamic range) mode. Metabolite standard samples of O-succinylhomoserine ([M+H]+m/z=220.0822, RT=7.77) methionine ([M+H]+m/z=150.5609, RT=8.28), S-adenosylmethionine (SAM) ([M+H]+m/z=400.1497, RT=17.1), S-adenosylhomocysteine (SAH) ([M+H]+m/z=386.3493, RT=13.36) and N-formyl-L-methionine ([M+H]+m/z=178.0543, RT=1.33) were dissolved at a range of concentrations in the same matrix solution as the bacterial samples (ACN:MeOH:H_2O; 2 : 2 : 1 v/v/v) and were run alongside the experimental samples for quantification purposes. Metabolite abundances were performed using Agilent's Mass Hunter suite and Mass Profinder software (Fig. S1). A standard curve of the ion count abundances of each standard metabolite versus its concentration was used for the quantification of the same metabolite in the experimental samples. Metabolite abundances were normalized with residual protein of each sample, which was estimated using a BCA protein assay kit (Pierce; 23225).

Chromatin immunoprecipitation (ChIP)

Cultures were grown in 3 mM NH_4Cl Gutnick minimal medium as above; 25 ml was sampled at N+, N− and N-24, and processed exactly as previously described by [5]. Either anti-FLAG (M2) or anti-β (WP002) antibodies were used for the MetJ-FLAG ChIP and RNAP ChIP, respectively. Primers used for rate limiting semi-quantitative PCR are listed in Table S2.

Statistical analysis

Unless otherwise specified, all data show the mean average of at least three independent experiments, where variation shown is the SEM. Statistical significance was determined using Student's *t*-test or one-way ANOVA where a probability (*P*) value of <0.05 was considered statistically significant (* $P<0.05$, ** $P<0.01$, *** $P<0.001$, NS – not significant).

RESULTS AND DISCUSSION

The initial 24 h of N starvation represents a physiologically important period during which YeaG-mediated adaptation to sustained N starvation occurs

To decipher the molecular basis by which YeaG contributes to adaptation to sustained N starvation, we began our study by measuring the intracellular levels of YeaG in whole-cell extracts from cells experiencing N starvation over 5 days. Results revealed that YeaG levels peaked within the first 24 h following entry into N starvation, but subsequently diminish (Fig. 1a). Although YeaG *per se* might be subject to regulation, this observation suggests that the YeaG-mediated adaptive response to N starvation occurs, at least under our conditions, within the first 24 h upon entry into N starvation. Further, since the viability of Δ*yeaG* bacteria gradually decreased only after 24 h under N starvation (N-24) (resulting in ~22 % of the mutant population surviving after 5 days under N starvation compared to the wild-type; Fig. 1b), the results imply that the initial 24 h of N starvation represents a physiologically important period during which YeaG-mediated adaptation to sustained N starvation happens.

The NtrC-mediated transcriptional response to N starvation is dynamic

We next compared the transcriptomes of wild-type and Δ*yeaG* bacteria during exponential growth under N replete conditions (N+), following the initial response to N starvation (20 min following N run-out; N−) and after experiencing 24 h of N starvation (N-24) to understand how YeaG contributes to adaptation to sustained N starvation. We defined differentially expressed genes as those with expression levels changed ≥twofold with a false-discovery-rate-adjusted *P*-value <0.05. The initial transcriptional response to N starvation involves the activation of genes required for scavenging of alternative N sources by NtrC [4, 5]. We therefore compared how the transcript levels of NtrC-activated genes (as defined in [5]) differed in wild-type and Δ*yeaG* bacteria at N− (compared to N+) and N-24 (compared to N− and N+). In wild-type bacteria, as expected, the transcript levels of the majority of NtrC-activated genes increased in response to N starvation at N− (Fig. 2a). Following sustained N starvation at N-24, the transcript levels of NtrC-activated genes become overall reduced (Fig. 2b), but remain elevated in comparison to N+ (Fig. 2c). We also note that the *rut* operon, which encodes proteins associated with pyrimidine degradation, becomes further upregulated during sustained N starvation (Fig. 2b, c). Consistent with this observation, NtrC was still present following 24 h of N starvation in both wild-type and Δ*yeaG* bacteria (Fig. 2d). Interestingly, we note that

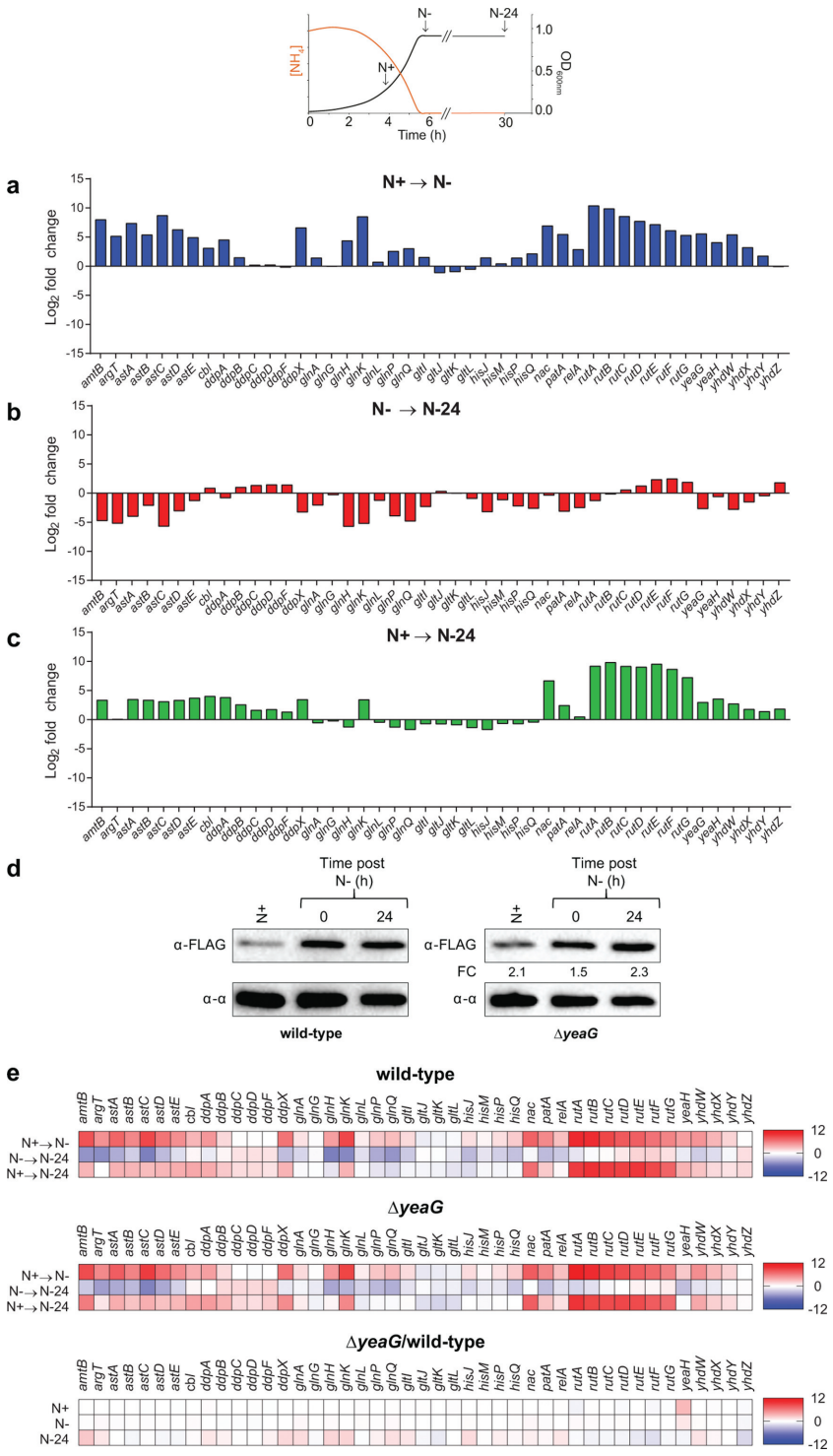

Fig. 2. The NtrC-mediated transcriptional response to N starvation is dynamic. (a–c) Log_2 fold change in mean expression of the 46 genes within the NtrC regulon [as described in (5)] for wild-type bacteria from N+ to N− (a), N− to N-24 (b) and N+ to N-24 (c). (d) Representative immunoblot of whole-cell extracts of bacterial cells sampled at N+, N− and N-24 in wild-type (left) and Δ*yeaG* (right) bacteria, probed with anti-FLAG antibody (to detect NtrC) and anti-RNA polymerase α subunit antibody (loading control). Fold change (FC) between NtrC levels in wild-type and Δ*yeaG* bacteria was calculated by obtaining the ratio in band intensities between the band corresponding to NtrC and the RNAP α subunit (loading control), and dividing the values obtained for Δ*yeaG* samples by the values obtained for the wild-type samples from the corresponding time point. The bands corresponding to NtrC and α subunit shown are from the same blot. (e) Heat maps showing the log_2 fold change in expression levels of the NtrC-regulated genes in wild-type (top) and Δ*yeaG* (middle) bacteria at N− relative to N+, N-24 relative to N−, and N-24 relative to N+, and in Δ*yeaG* relative to wild-type bacteria at N+,

N−, and N-24 (bottom). The colour keys on the right indicate the range in fold change in relative gene expression for each comparison. The schematic representation of the bacterial growth curve at the top indicates the time points: N+, N− and N-24 with respect to the N consumption ($[NH_4]$) and growth ($OD_{600\ nm}$).

the intracellular level of NtrC at N-24 was ~twofold higher in Δ*yeaG* bacteria compared to wild-type bacteria at N+, N− and N-24. Since the transcript levels of *glnG*, the gene encoding for NtrC do not significantly differ in wild-type and mutant samples, we consider it possible that NtrC is subject to post-transcriptional regulation. We next considered whether the expression of the NtrC-activated genes becomes dysregulated in the absence of YeaG. As shown in the heat maps of genes differentially expressed in wild-type and Δ*yeaG* bacteria (Fig. 2e), the absence of YeaG does not substantially change the expression profile of NtrC-activated genes at N− or N-24. Overall, it seems that the NtrC-mediated transcriptional response to N starvation is dynamic and possibly subject to temporal regulation. It further seems that the expression of the NtrC-activated genes does not substantially differ between wild-type and Δ*yeaG* bacteria in the initial response to N starvation (N-) and following sustained N starvation (N-24).

Δ*yeaG* bacteria experiencing sustained N starvation have subtle dysregulation of the σ^{38} regulon

In our previous work [6], we used qRT-PCR to establish that the transcript levels of two toxin/antitoxin (TA) modules: *mqsR/mqsA* and *dinJ/yafQ*, were upregulated (by ~four and ~threefold, respectively) in Δ*yeaG* bacteria compared to wild-type bacteria following sustained N starvation (at N-24). The *mqsR/mqsA* TA module directly represses the transcription of σ^{38} [19, 20]. Similarly, DinJ, the toxin component of the *dinJ/yafQ* TA module, has been implicated in reducing σ^{38} levels through directly repressing the transcription of *cspE*, which in turn positively affects σ^{38} translation through stabilization of *rpoS* mRNA [21]. Consistent with our previous observations, analysis of the relative transcript levels of *mqsR*, *mqsA*, *dinJ* and *yafQ* in the transcriptome of Δ*yeaG* bacteria at N-24 was upregulated compared to wild-type bacteria; conversely, transcript levels of *cspD* and *cspE* were lower (Fig. S2a). However, none of these (except for *cspD*) differences were statistically significant based on the cut-off criteria of the RNA-seq data analysis (see above). Nevertheless, and consistent with previous observations [6], the protein levels of σ^{38} were reduced by 1.9 and >fourfold in Δ*yeaG* bacteria compared to wild-type bacteria at N− and N-24, respectively (Fig. S2b). Therefore, we considered whether dysregulated expression of the σ^{38} regulon (as defined by [8]) could be a reason for the compromised ability of the Δ*yeaG* bacteria to survive sustained N starvation. As seen with the NtrC-activated genes (Fig. 2a–c), in wild-type bacteria, the transcript levels of σ^{38}-dependent genes were upregulated at N−. Following sustained N starvation, at N-24, the transcript levels of these genes become overall reduced but remain higher still than at N+ (Fig. S2c). This observation further underscores the view that the transcriptome of *E. coli* experiencing sustained N starvation is dynamic. As shown in Fig. 3(a, b), none of the σ^{38}-dependent genes were differentially expressed in Δ*yeaG* bacteria at N+ (except *yeaH*; see later) and N−. However, a small subset (9/113; ~8 %) of the σ^{38}-dependent genes were differentially expressed at N-24 (Fig. 3c). Of these nine genes, the biological roles of six (*eutH, yciG, yebf, ygbA, yjdc* and *ymgA*) are unknown; whereas the remaining three (*amyA, narU* and *yfcF*) have diverse functions (amylase, nitrate/nitrite transporter and glutathione S-transferase, respectively). Overall, although we cannot exclude a role for these nine σ^{38}-dependent genes in adaptation to sustained N starvation, it seems that, despite σ^{38} levels being >fourfold lower, the σ^{38} regulon is only subtly dysregulated in Δ*yeaG* bacteria.

A role for YeaG in regulating motility-associated gene expression during the initial adaptive response to N starvation

We generated volcano plots to compare the complete transcriptomes of wild-type and Δ*yeaG* bacteria at N+, N− and N-24 (Fig. 4a–c). A total of 21 and 199 genes were differentially expressed in Δ*yeaG* bacteria compared to the wild-type at N− and N-24, respectively (Fig. 4b, c, Tables S3 and S4). As above (Fig. 3a), only *yeaH* appears differentially expressed at N+ in Δ*yeaG* bacteria compared to the wild-type (Fig. 4a). Further, analysis of the transcript levels of *yeaH* by qRT-PCR at N+, N− and N-24 showed that *yeaH* transcripts were increased by ~fivefold in Δ*yeaG* bacteria compared to wild-type bacteria at N+ but expressed to identical levels at N− and N-24 (Fig. S3, and also see Fig. 4b, c and Tables S3 and S4). We cannot conclusively explain why *yeaH* transcript levels are increased at N+ but not at N− or N-24 in Δ*yeaG* bacteria, however, we are confident that the properties of Δ*yeaG* bacteria described below are solely due to the absence of *yeaG* (and unlikely due to the dysregulation of *yeaH*) as the properties of mutant bacteria described can be complemented (see Fig. S5 later). Categorization of differentially expressed genes using Clusters of Orthologous Groups (COG) analysis [22] revealed that the majority of upregulated genes at N− in Δ*yeaG* bacteria were associated with the biosynthesis of flagella and motility (*fliC*, *fliD*, *motA*, *motB*, *tap*, *tar*, *tsr*, *fimI* and *flgK*) (Fig. 4d and Table S3). Spinning of *E. coli* cells is indicative of the presence of functional flagella when tethered to a glass surface. Therefore, we examined samples of Δ*yeaG* and wild-type bacteria from N− by phase-contrast microscopy. As shown in Movie S1 ('MP4, 71.47 Kb' in the supplementary material), we failed to detect any spinning cells in the wild-type sample. In contrast, the Δ*yeaG* sample contained several spinning and motile cells (Movie S2 – 'MP4, 71.95Kb' in the supplementary material). Interestingly, however, in

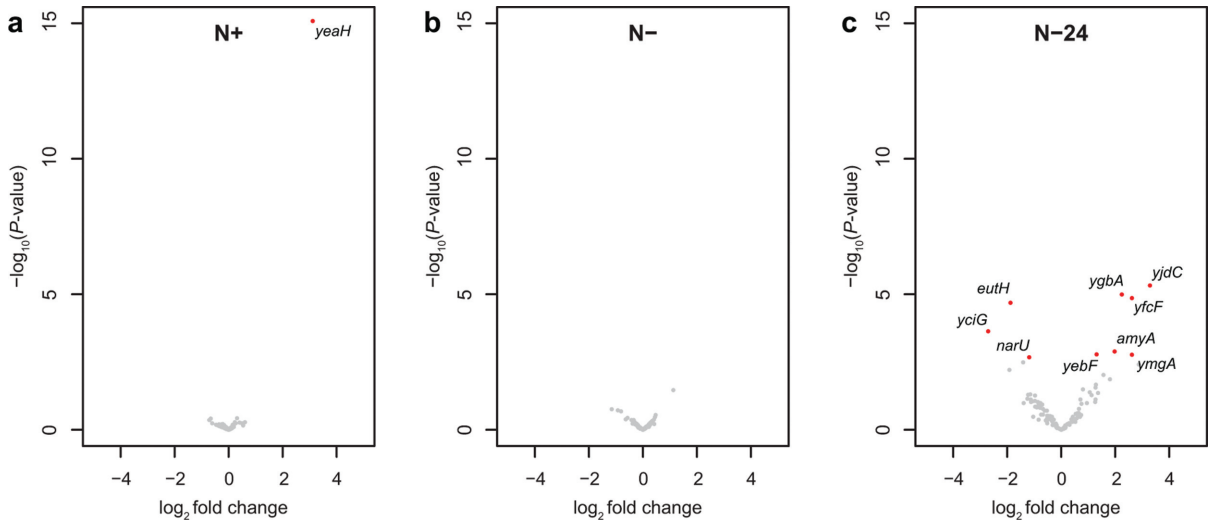

Fig. 3. Δ*yeaG* bacteria experiencing sustained N starvation have subtle dysregulation of the σ^{38} regulon. (a–c) Volcano plots revealing expression levels of all genes within the σ^{38} regulon at N+, N− and N-24 (for (a), (b) and (c), respectively) in Δ*yeaG* bacteria as a $\log_2$ fold change from wild-type, where red indicates differentially expressed genes changed ≥twofold with a false-discovery-rate-adjusted *P*-value <0.05.

Movie S2 we note that ~2 % of the Δ*yeaG* cells were spinning or motile, while most cells resembled wild-type bacteria, suggesting that the upregulation of motility genes in the Δ*yeaG* population at N− could occur in a heterogeneous manner. We further note that the motility-associated genes in Δ*yeaG* bacteria are downregulated to near wild-type levels at N-24 (Fig. S4), suggesting that dysregulation of these genes in Δ*yeaG* bacteria is a property of mutant bacteria that is specific to the initial adaptive response to N starvation. We thus conclude that YeaG could have a role in the regulation of motility-associated gene expression during the initial adaptive response to N starvation.

A role for YeaG in regulating methionine biosynthesis genes in *E. coli* experiencing sustained N starvation

Since the viability of the Δ*yeaG* population begins to decline after 24 h under N starvation, we next focused on differences in the transcriptomes of wild-type and Δ*yeaG* bacteria at N-24. COG analysis of differentially expressed genes at N-24 revealed that the majority of upregulated genes were either uncharacterized or associated with amino acid transport and metabolism, and of the latter group, genes involved in the biosynthesis of methionine were most highly upregulated (Fig. 4c, e and Table S4). Conversely, genes associated with coenzyme transport and metabolism, and particularly NAD^+ biosynthesis, were most highly downregulated (Fig. 4c, e and Table S4). Interestingly, aspartate serves as the precursor for both NAD^+ and methionine biosynthesis, thus the data suggests that aspartate becomes preferentially directed towards methionine biosynthesis in Δ*yeaG* cells at N-24.

In *E. coli*, the transcription of methionine biosynthesis genes is under negative regulation by MetJ. In wild-type bacteria, when cells become nitrogen starved (i.e. when they transition from N+ to N-), the transcript levels of genes within the MetJ regulon decreased. This response occurs in Δ*yeaG* bacteria to a similar extent (Fig. 5a). However, during sustained nitrogen starvation (i.e. when the cells transition from N− to N-24), a subset of these genes become upregulated in both wild-type and mutant bacteria (Fig. 5b), consistent with the view that the transcriptome of *E. coli* experiencing N starvation is dynamic. Strikingly, in Δ*yeaG* bacteria, the magnitude by which this upregulation occurred was substantially higher compared to the wild-type (Fig. 5b, c, and Table S4). Quantification of transcript levels of the most dysregulated genes in Δ*yeaG* bacteria (*artJ*, *metA*, *metB*, *metF*, *metR*, *mmuP*, *nadA*, *nadB*, *pnuC,* and *yhdV*) by qRT-PCR in wild-type, Δ*yeaG* bacteria and Δ*yeaG* bacteria in which *yeaG* was complemented from an inducible plasmid, validated the RNA-seq data and confirmed that the differences in transcript levels were due to the absence of *yeaG* (Fig. S5). Overall, we conclude that YeaG has a role in the transcriptional regulation of methionine biosynthesis genes in *E. coli* experiencing sustained N starvation. Further, *metA, metB, metF, metR,* and *mmuP* displayed similar levels of upregulation in Δ*yeaH* and Δ*yeaGH* bacteria as in Δ*yeaG* bacteria at N-24 (Fig. S6), underscoring previous observations that YeaG and YeaH functionally interact [6].

Aberrant activation of the methionine biosynthesis pathway after 24 h in N starved Δ*yeaG* bacteria

As synthesis of one methionine molecule in *E. coli* requires seven molecules of ATP [23], we thus considered whether the aberrant synthesis of methionine and associated

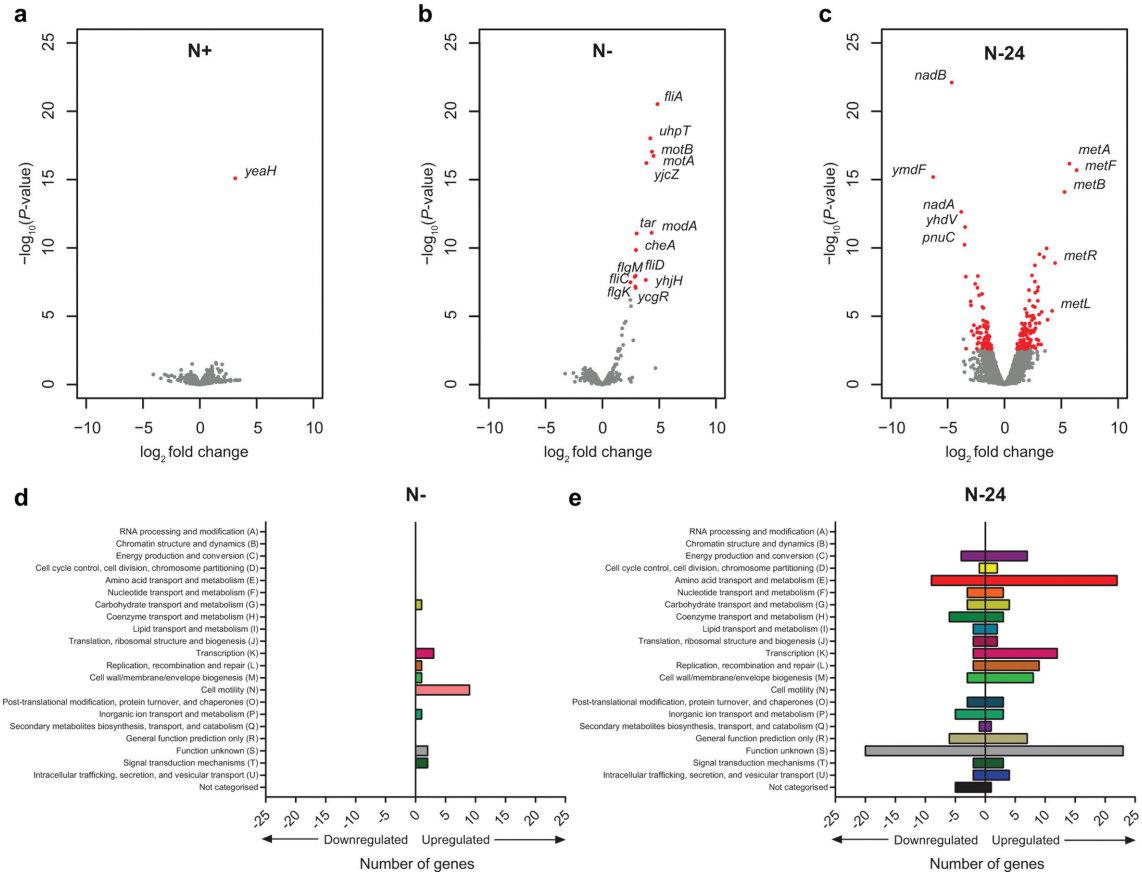

Fig. 4. A role for YeaG in regulating motility-associated gene expression during the initial adaptive response to N starvation. (a–c) Volcano plots revealing expression levels of all genes at N+, N− and N-24 (for (a), (b) and (c) respectively) in Δ*yeaG* bacteria as a $\log_2$ fold change from wild-type, where red indicates differentially expressed genes changed ≥twofold with a false-discovery-rate-adjusted *P*-value <0.05. The identities of genes that are most differentially expressed and relevant to the study are provided and shown in red. (d) Graph categorizing all differentially expressed genes at N− based on their COG annotation. (e) As in (d) but for N-24.

metabolites of the pathway in Δ*yeaG* bacteria compromises the viability of the mutant population after 24 h under N starvation. We used liquid chromatography-electrospray ionization mass spectrometry metabolomics to carry out a targeted analysis of selected intermediates [O-succinylhomoserine, methionine, S-adenosylmethionine (SAM) and S-adenosylhomocysteine (SAH)] associated with the methionine biosynthesis pathway in wild-type and Δ*yeaG* bacteria at N+, N− and N-24. The intracellular levels of the measured metabolites did not significantly differ between the wild-type and Δ*yeaG* bacteria at N+ and N− (Fig. 6). However, at N−, the intracellular levels of the measured metabolites were overall lower than at N+ (Fig. 6). Consistent with the differences in the transcription of methionine biosynthesis genes between wild-type and Δ*yeaG* bacteria at N-24 (Figs 4c and 5, Table S4), the intracellular levels of O-succinylhomoserine, methionine, SAM and SAH were higher in Δ*yeaG* cells than in the wild-type at N-24 (Fig. 6). We note that levels of N-formylmethionine, the initiating amino acid for most proteins, are similar in wild-type and Δ*yeaG* at N-24, suggesting that methionine is routed towards the SAM cycle in Δ*yeaG* bacteria. Overall, the results unambiguously confirm that the methionine biosynthesis pathway is active and aberrantly upregulated in Δ*yeaG* bacteria following 24 h of N starvation.

Transcriptional derepression leads to activation of the methionine biosynthesis pathway in 24 h N starved Δ*yeaG* bacteria

Most of the methionine biosynthesis genes that become dysregulated at N-24 in Δ*yeaG* bacteria are negatively regulated by the transcription repressor, MetJ, along with its cofactor, SAM, which increases the affinity of MetJ to bind cognate sites by ~100–1000-fold [24]. Although intracellular SAM levels are ~threefold higher and *metJ* transcript levels are ~eightfold higher in Δ*yeaG* cells compared to wild-type cells at N-24 (Fig. 6 and Table S4 respectively), somewhat paradoxically, it seems that MetJ activity becomes compromised in mutant bacteria during sustained N starvation. We thus

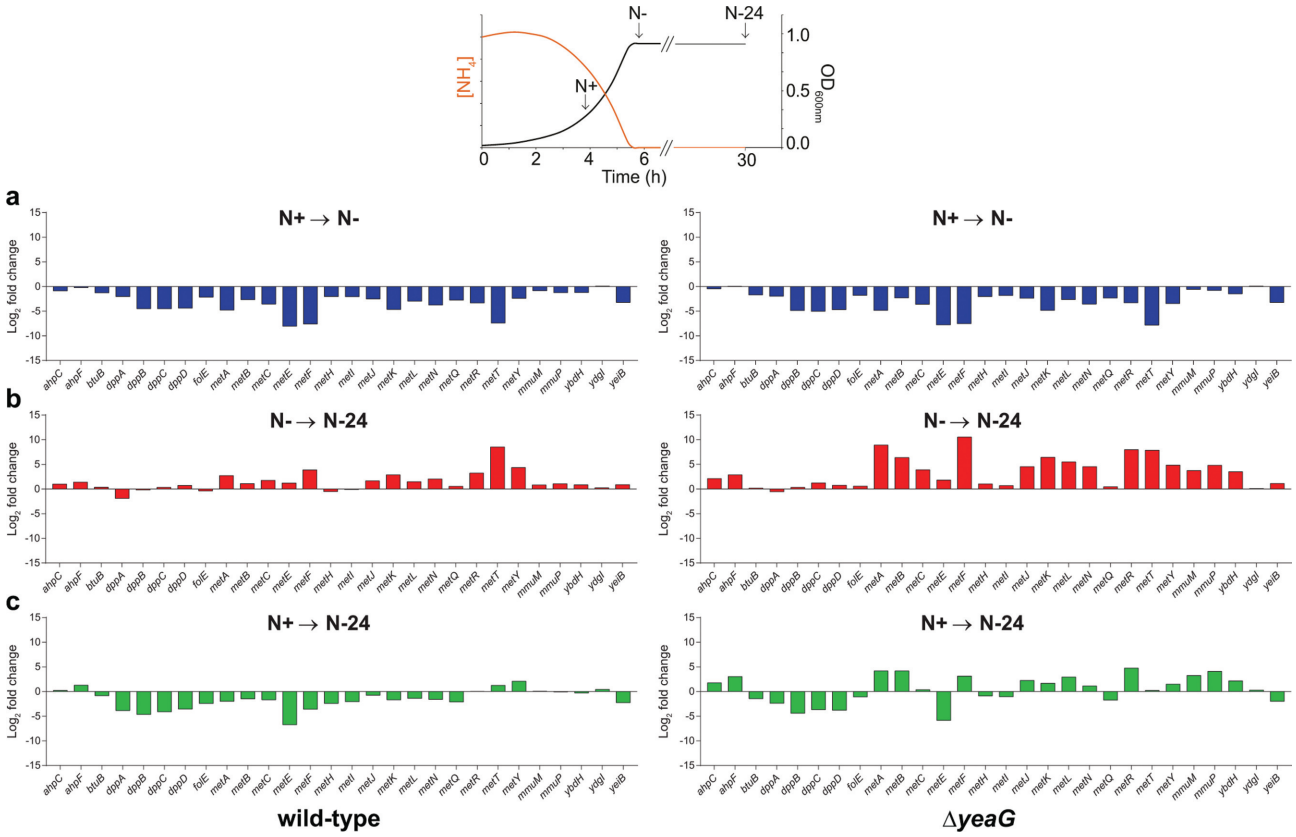

Fig. 5. A role for YeaG in regulating methionine biosynthesis genes in *E. coli* experiencing sustained N starvation. Graphs showing the $\log_2$ fold change in expression levels of genes of the MetJ regulon [as defined by (15)] in wild-type (left) and Δ*yeaG* (right) bacteria at N− relative to N+ (a), N-24 relative to N− (b), and N-24 relative to N+ (c). The schematic representation of the bacterial growth curve at the top indicates the time points: N+, N− and N-24 with respect to the N consumption ($[NH_4]$) and growth ($OD_{600\ nm}$).

considered whether either the stability or the affinity of MetJ to bind its cognate binding sites (called met boxes) found upstream of MetJ-repressed genes (or both) might be altered in Δ*yeaG* bacteria under sustained N starvation. To investigate whether the stability of MetJ is affected during the initial 24 h under N starvation in Δ*yeaG* bacteria, we introduced an in-frame fusion encoding three repeats of the FLAG epitope at the 3′ end of MetJ in wild-type and Δ*yeaG* bacteria. Initially, we confirmed that the presence of the FLAG epitope did not adversely affect the activity of the MetJ protein by comparing the relative levels of *metF* transcripts (a gene which contains five met boxes and thus, is heavily repressed by MetJ in the presence of excess methionine; Fig. 7a) in wild-type, Δ*metJ*, wild-type *metJ*-FLAG and Δ*yeaG metJ*-FLAG strains grown in LB broth supplemented with 100 μg ml^{-1} methionine. As shown in Fig. 7(b), the FLAG epitope did not detectably affect the activity of MetJ. We then used an antibody against the FLAG epitope to measure the relative intracellular levels of MetJ-FLAG protein in whole-cell extracts prepared from wild-type *metJ*-FLAG and Δ*yeaG metJ*-FLAG cells as a function of time (up to 24 h) under N starvation. Results shown in Fig. 7(c) reveal that the intracellular levels of MetJ-FLAG protein in wild-type *metJ*-FLAG and Δ*yeaG metJ*-FLAG cells do not sufficiently differ to warrant the increased levels of *metF* transcription (and by inference, transcription of other MetJ-controlled genes) in the Δ*yeaG* bacteria at N-24. In fact, we note that the intracellular level of MetJ-FLAG protein is ~1.6-fold higher in Δ*yeaG* bacteria than wild-type bacteria at N-24.

We next investigated whether the affinity of MetJ to bind to the met boxes is adversely affected in Δ*yeaG* bacteria at N-24. To do so, we used chromatin immunoprecipitation to obtain MetJ-FLAG bound DNA fragments using anti-FLAG antibodies and subsequent rate-limiting semi-quantitative PCR for specific enrichment of a MetJ binding sequence. To overcome the limited sensitivity of this method, we chose to enrich the *metF* regulatory region because *metF* (i) is the only MetJ repressed gene that contains five met boxes (Fig. 7a), (ii) is highly de-repressed in our RNA-seq analysis in Δ*yeaG* bacteria (Fig. 4c and Table S4), and (iii) is widely used for *in vitro* analyses of MetJ-DNA interactions [24, 25]. As shown in Fig. 7(d), the binding of MetJ to the *metF* regulatory region in Δ*yeaG* bacteria was only slightly decreased (by ~1.3- (at N−) and ~1.5- (at N-24) fold)

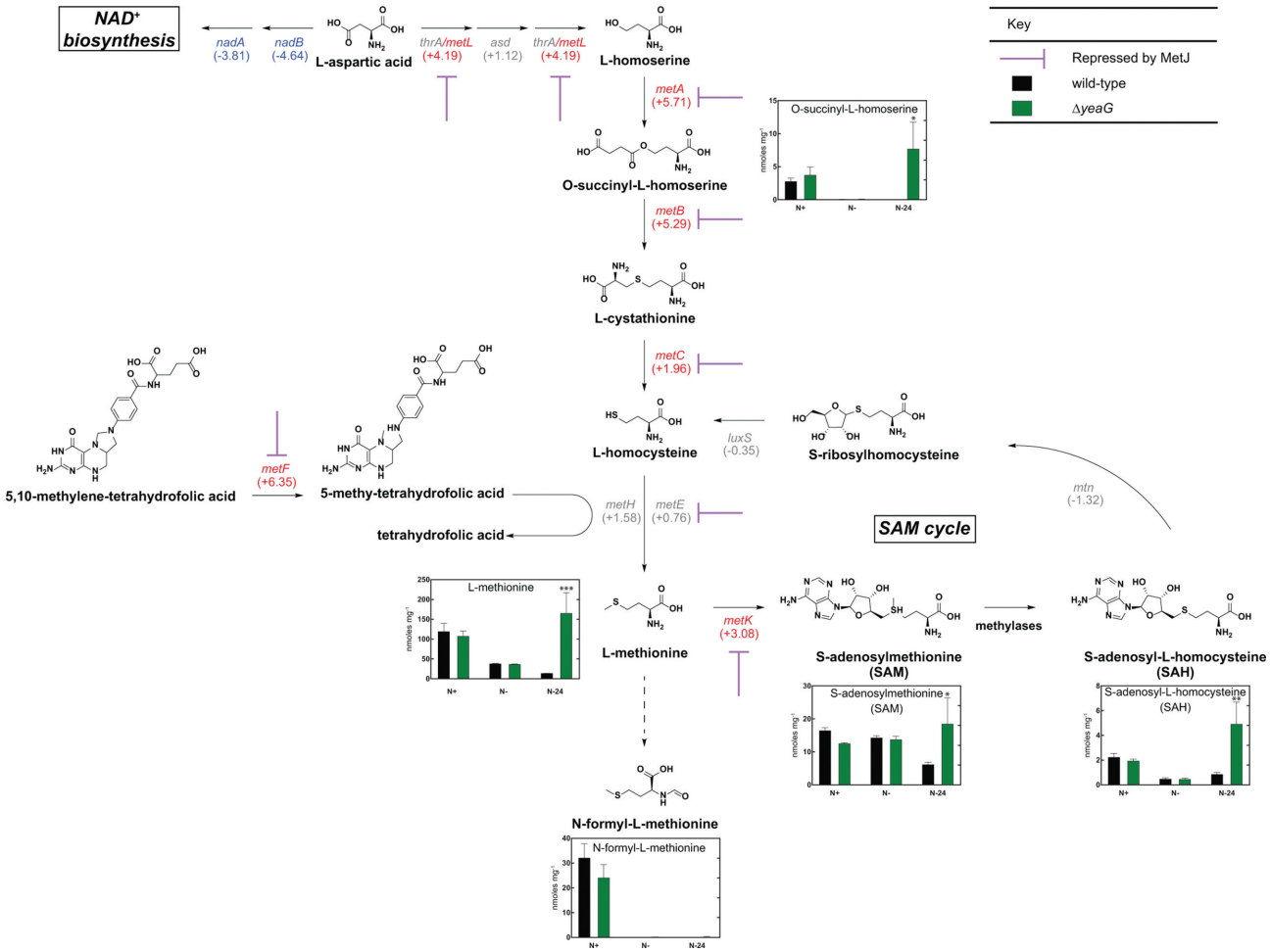

Fig. 6. Aberrant activation of the methionine biosynthesis pathway after 24 h in N starved Δ*yeaG* bacteria. Schematic outlining the methionine biosynthesis pathway in *E. coli*. The purple bars indicate genes that are repressed by MetJ. The numbers in parentheses represent the $\log_2$ fold change in gene expression in Δ*yeaG* relative to wild-type bacteria at N-24 for the associated gene. The concentrations of measured metabolites (nmoles mg^{-1}) associated with methionine biosynthesis in either wild-type or Δ*yeaG* bacteria at N+, N− and N-24 are represented in bar charts. Error bars represent SEM (n=3). Statistical analyses were performed by one-way ANOVA (* P<0.05, ** P<0.01, ***P<0.001).

(compare lane 5 with 14 and 8 with 17, respectively), suggesting that the affinity of MetJ to bind the met boxes is only subtly compromised in Δ*yeaG* bacteria compared to wild-type bacteria. Since the met boxes at most MetJ controlled promoters (as predicted or experimentally validated on EcoCyc – www.ecocyc.org) are located with respect to the core promoter sequences (i.e. −35 and −10 regions) such that MetJ binding would occlude RNAP binding, we immunoprecipitated RNAP and repeated the experiment described in Fig. 7(d) to determine how efficiently RNAP bound to the *metF* promoter in wild-type and mutant bacteria. As shown in Fig. 7(e), a ~4.8-fold increase in RNAP binding to the *metF* promoter was detected in Δ*yeaG* bacteria compared to wild-type bacteria at N-24 (compare lanes 2 and 4). It thus seems that, despite MetJ being present at the *metF* promoter, and by extension, other MetJ-repressed promoters, RNAP can access and initiate transcription from these promoters in Δ*yeaG* bacteria at N-24. Overall, we conclude that the aberrant upregulation of methionine biosynthesis genes in Δ*yeaG* bacteria at N-24 occurs because MetJ is unable to effectively prevent RNAP from accessing the promoter, thus leading to transcriptional derepression of MetJ-regulated genes.

Transcriptional dysregulation of methionine biosynthesis genes does not appear to be a contributing factor for compromised viability of Δ*yeaG* bacteria experiencing sustained N starvation

Since MetJ-repressed genes clearly become upregulated in Δ*yeaG* bacteria experiencing sustained N starvation, resulting in the aberrant biosynthesis of methionine and associated intermediates, we considered whether this energetically

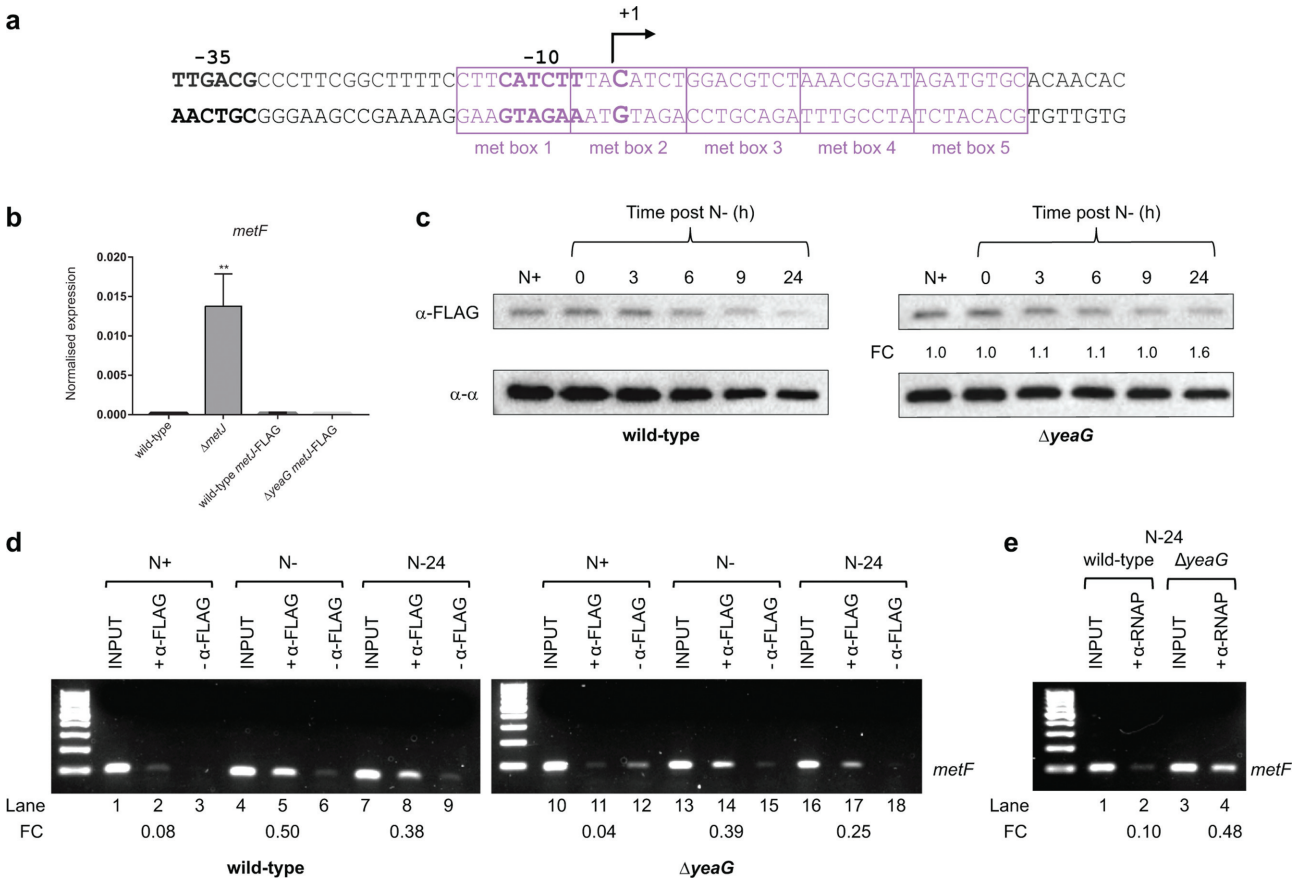

Fig. 7. Derepression of transcription leads to activation of the methionine biosynthesis pathway in 24 h N starved Δ*yeaG* bacteria. (a) The sequence of the *metF* promoter showing the −35 and −10 promoter regions with respect to the transcription start site (+1). Boxed in purple are the met boxes. (b) Graph showing qRT-PCR results of relative abundance of *metF* transcripts in wild-type, Δ*metJ*, wild-type *metJ*-FLAG and Δ*yeaG metJ*-FLAG cells normalized to 16S rRNA internal control (see text for details). Error bars represent SEM (n=3). Statistical analyses were performed by one-way ANOVA (** P<0.01). (c) Representative immunoblot of whole-cell extracts of bacterial cells sampled at N+ and following various periods of N starvation, probed with anti-FLAG antibody (to detect MetJ) and anti-RNA polymerase alpha subunit antibody (loading control). Fold change (FC) between MetJ levels in wild-type and Δ*yeaG* bacteria was calculated by obtaining the ratio in band intensities between the band corresponding to MetJ and the RNAP α subunit (loading control), and dividing the values obtained for Δ*yeaG* samples by the values obtained for the wild-type samples from the corresponding time point. The bands corresponding to MetJ and α subunit shown are from the same blot, where different blots were used for samples from wild-type and Δ*yeaG* bacteria; both blots were exposed and processed at the same time. (d) Representative image of an agarose gel showing PCR products corresponding to the *metF* promoter region in the N+, N− and N-24 samples immunoprecipitated with anti-FLAG antibodies, i.e. bound by MetJ (see text for details). (e) As in (d) but anti-β antibodies were used to immunoprecipitate RNAP bound to the *metF* promoter region at N+, N− and N-24. In (d) and (e), FC indicates fold change in band intensity of the signal corresponding to the *metF* promoter region relative to the input positive control sample.

costly process is a contributing factor towards the compromised viability of Δ*yeaG* bacteria experiencing sustained N starvation. To investigate this, we compared the viability of Δ*yeaG*, Δ*metJ* and Δ*yeaG*Δ*metJ* bacteria at N− and following 5 days under N starvation with that of wild-type bacteria by counting viable c.f.u. No difference in the viability was detected for Δ*yeaG*, Δ*metJ* and Δ*yeaG*Δ*metJ* bacteria compared to wild-type bacteria at N− (data not shown). Consistent with the data shown in Fig. 1(b), the viability of Δ*yeaG* and Δ*yeaG*Δ*metJ* bacteria decreased by ~58 and ~46 %, respectively, compared to wild-type bacteria following 5 days under N starvation (Fig. 8). However, surprisingly, the viability of Δ*metJ* was slightly higher than that of wild-type bacteria (~127 %) following 5 days under N starvation. Overall, we conclude that the transcriptional dysregulation of methionine biosynthesis genes, and the consequential aberrant biosynthesis of methionine, is not a contributing factor for the compromised viability of Δ*yeaG* bacteria experiencing sustained N starvation.

Conclusions

Many bacterial adaptive responses begin with, and are accompanied by, large-scale changes to the transcriptome.

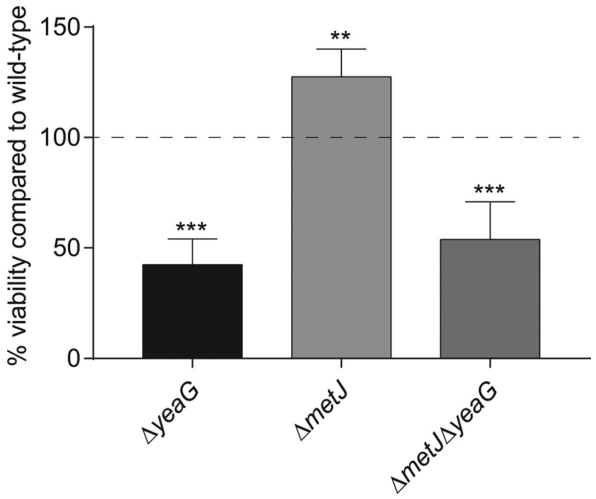

Fig. 8. Transcriptional dysregulation of methionine biosynthesis genes does not appear to be a contributing factor for compromised viability of Δ*yeaG* bacteria experiencing sustained N starvation. Bar chart showing the viability of Δ*yeaG*, Δ*metJ* and Δ*metJ*Δ*yeaG* bacteria as measured by counting c.f.u. after 5 days under sustained N starvation. Bars show percentage viability of each strain compared to the wild-type. Error bars represent SEM (n=3). Statistical analyses were performed by one-way ANOVA (** P<0.01, ***P<0.001).

The coordination and the scale of the changes that occur in the transcriptome are often underpinned by multiple and complex control layers, which ensure the appropriateness of the adaptive response to benefit the cell. The initial adaptive transcriptional response to N starvation in *Escherichia coli* and related bacteria is orchestrated by the global transcription factor, NtrC. This initial response, which is energetically costly, allows the cells to adjust their physiology to actively import and assimilate N from alternative resources. How the transcriptome changes and the regulatory basis underpinning such changes during sustained N starvation however, are not well understood. Although expression of the NtrC regulon does not considerably differ between wild-type and Δ*yeaG* bacteria, the results of this study indicate that the transcriptome of *E. coli* experiencing sustained N starvation is likely to be dynamic and subject to temporal regulation. Surprisingly, despite σ^{38} levels being clearly lower in Δ*yeaG* bacteria compared to wild-type bacteria at N-24, our transcriptomics data show that the σ^{38} regulon is only subtly differentially expressed in Δ*yeaG* bacteria.

The initial adaptive response to N starvation is largely a scavenging response and does not involve chemotactic-like behaviour [26]. Intriguingly, some cells in the Δ*yeaG* population synthesize functional flagella and display motility upon entry into N starvation. This observation implies a potential role for YeaG in regulating flagellum biosynthesis genes and motility during the *initial* adaptive response to N starvation, which warrants further investigation. We further note that a study by Dong *et al.* [27] revealed that a Δ*rpoS E. coli* strain displays enhanced motility due to the increased

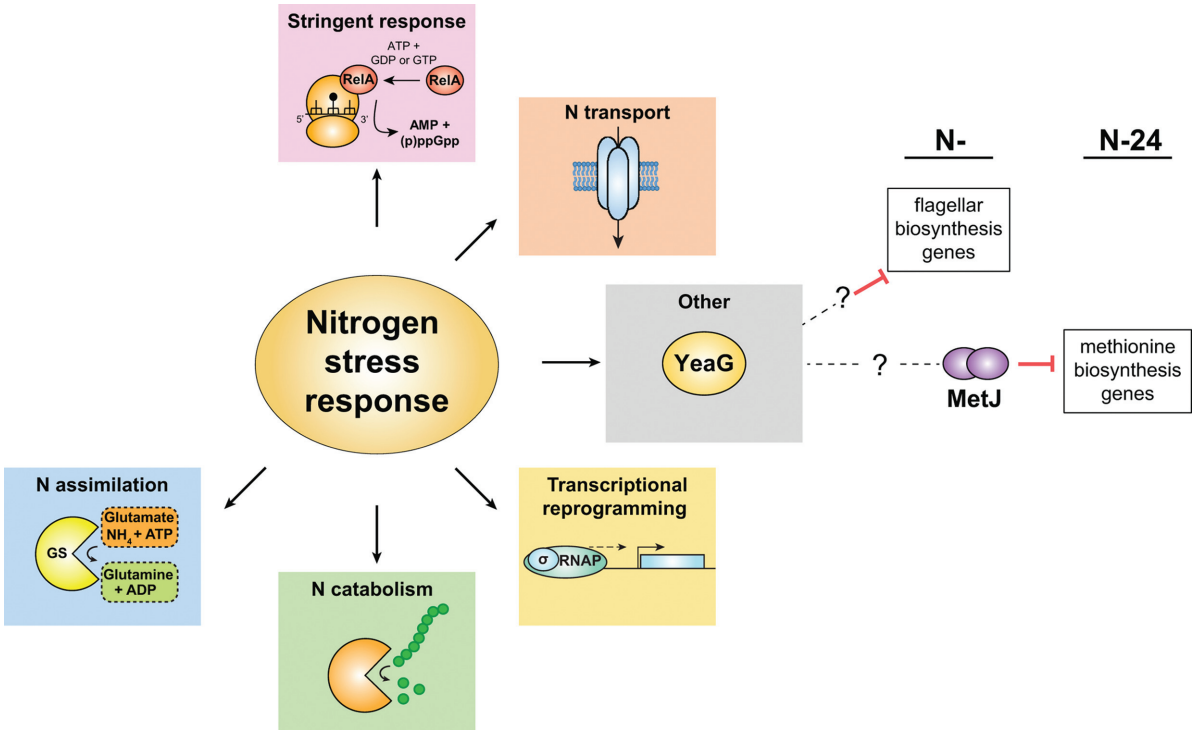

Fig. 9. Model proposing that the *yeaGH* operon represents a new branch within the nitrogen stress response in *E. coli*.

expression of FliA (the RNAP σ factor associated with the transcription of motility-associated genes, including those upregulated in Δ*yeaG* bacteria at N−; Fig. 4d and Table S3). Thus, it is possible that the increased motility of the ΔyeaG bacteria at N− is somehow connected to the reduction in σ38 levels in ΔyeaG bacteria at N-24 (Fig. 3a). However, it is unlikely to be the case since motility genes are not differentially expressed at N-24.

We have uncovered that YeaG is part of the regulatory sub-circuit controlling the expression of methionine biosynthesis genes in sustained N starved *E. coli* and furthermore, have demonstrated that the absence of YeaG results in transcriptional derepression of these genes and subsequent activation of the methionine biosynthesis pathway. It appears that YeaG is required for the ability of MetJ to fully repress the transcription of genes within its regulon in *E. coli* experiencing *sustained* N starvation. Strikingly, however, the aberrant activation of the methionine biosynthesis pathway is not a contributing factor for the decreased viability of Δ*yeaG* bacteria experiencing sustained N starvation.

We note that the intracellular levels of SAM are ~threefold higher in Δ*yeaG* bacteria compared to wild-type bacteria at N-24. SAM is generated from methionine and ATP to be used as a major cofactor (reviewed in [28]) within the cell, and an important nucleoside serving as a methyl donor in a broad array of metabolic and biosynthetic reactions, including methylation of DNA, RNA, proteins and lipids. Methylation can have direct biochemical relevance in metabolic reactions and is involved in transcription regulation at the epigenetic level. Thus, it is tantalizing to speculate whether epigenetic control of the transcriptome, through methylation or phosphorylation, happens during sustained N starvation and the role of YeaG in this process. In other words, based on our data that YeaG affects the transcriptome of *E. coli* experiencing N starvation, we hypothesize that dysregulated epigenetic control of the transcriptome in the absence of YeaG could adversely affect the viability of *E. coli* experiencing sustained N starvation.

In summary, we consider that the *yeaGH* operon represents a new branch in the transcriptional response to N starvation in *E. coli* and related bacteria (Fig. 9). Although the transcriptional responses to transient growth arrests or during growth transitions due to nutrient starvation (e.g. diauxic growth) has been previously explored, this study uniquely demonstrates that the transcriptome of growth attenuated bacteria experiencing sustained nutrient starvation is plastic, and in the case of the N stress response, this plasticity is affected by the kinase, YeaG.

Funding information
A Wellcome Trust Investigator award WT100958MA and an MRC doctoral studentship funded this work. Work in the L.P.S.C laboratory was supported by the Francis Crick Institute, which receives its core funding from Cancer Research UK (FC001060), the UK Medical Research Council (FC001060), and the Wellcome Trust (FC001060). L.P.S.C's laboratory also acknowledges funds from a Wellcome Trust New Investigator Award (104785/B/14/Z).

Acknowledgements
We thank members of the S. W. laboratory for constructive comments on the manuscript.

Conflicts of interest
The authors declare that there are no conflicts of interest.

References

1. Hagan EC, Lloyd AL, Rasko DA, Faerber GJ, Mobley HL. *Escherichia coli* global gene expression in urine from women with urinary tract infection. *PLoS Pathog* 2010;6:e1001187.
2. Klose KE, Mekalanos JJ. Simultaneous prevention of glutamine synthesis and high-affinity transport attenuates *Salmonella* typhimurium virulence. *Infect Immun* 1997;65:587–596.
3. Ni J, Shen TD, Chen EZ, Bittinger K, Bailey A *et al.* A role for bacterial urease in gut dysbiosis and Crohn's disease. *Sci Transl Med* 2017;9:eaah6888.
4. Brown DR, Barton G, Pan Z, Buck M, Wigneshweraraj S. Combinatorial stress responses: direct coupling of two major stress responses in *Escherichia coli*. *Microb Cell* 2014;1:315–317.
5. Brown DR, Barton G, Pan Z, Buck M, Wigneshweraraj S. Nitrogen stress response and stringent response are coupled in *Escherichia coli*. *Nat Commun* 2014;5:4115.
6. Figueira R, Brown DR, Ferreira D, Eldridge MJ, Burchell L *et al.* Adaptation to sustained nitrogen starvation by *Escherichia coli* requires the eukaryote-like serine/threonine kinase YeaG. *Sci Rep* 2015;5:17524.
7. Zimmer DP, Soupene E, Lee HL, Wendisch VF, Khodursky AB *et al.* Nitrogen regulatory protein C-controlled genes of *Escherichia coli*: scavenging as a defense against nitrogen limitation. *Proc Natl Acad Sci USA* 2000;97:14674–14679.
8. Weber H, Polen T, Heuveling J, Wendisch VF, Hengge R. Genome-wide analysis of the general stress response network in *Escherichia coli*: sigmaS-dependent genes, promoters, and sigma factor selectivity. *J Bacteriol* 2005;187:1591–1603.
9. Rozen Y, Belkin S. Survival of enteric bacteria in seawater. *FEMS Microbiol Rev* 2001;25:513–529.
10. Gyaneshwar P, Paliy O, McAuliffe J, Popham DL, Jordan MI *et al.* Sulfur and nitrogen limitation in *Escherichia coli* K-12: specific homeostatic responses. *J Bacteriol* 2005;187:1074–1090.
11. Tagourti J, Landoulsi A, Richarme G. Cloning, expression, purification and characterization of the stress kinase YeaG from *Escherichia coli*. *Protein Expr Purif* 2008;59:79–85.
12. Stancik IA, Šestak MS, Ji B, Axelson-Fisk M, Franjevic D *et al.* Serine/Threonine protein kinases from bacteria, archaea and eukarya share a common evolutionary origin deeply rooted in the tree of life. *J Mol Biol* 2018;430:27–32.
13. Lee DJ, Bingle LE, Heurlier K, Pallen MJ, Penn CW *et al.* Gene doctoring: a method for recombineering in laboratory and pathogenic *Escherichia coli* strains. *BMC Microbiol* 2009;9:252.
14. Atlas RM. *Handbook of Microbiological Media*, 4th ed. Boca Raton, FL, USA: CRC Press; 2010.
15. Marincs F, Manfield IW, Stead JA, McDowall KJ, Stockley PG. Transcript analysis reveals an extended regulon and the importance of protein-protein co-operativity for the *Escherichia coli* methionine repressor. *Biochem J* 2006;396:227–234.
16. Sambrook JF, Russell DW. *Molecular Cloning: A Laboratory Manual*, 3rd ed. Cold Spring Harbor, New York: Cold Spring Harbor Lab Press; 2001. pp. 1–3.
17. Sarkar P, Switzer A, Peters C, Pogliano J, Wigneshweraraj S. Phenotypic consequences of RNA polymerase dysregulation in *Escherichia coli*. *Nucleic Acids Res* 2017;45:11131–11143.
18. Larrouy-Maumus G, Biswas T, Hunt DM, Kelly G, Tsodikov OV *et al.* Discovery of a glycerol 3-phosphate phosphatase

reveals glycerophospholipid polar head recycling in *Mycobacterium tuberculosis*. *Proc Natl Acad Sci USA* 2013;110:11320–11325.

19. **Kim Y, Wang X, Zhang XS, Grigoriu S, Page R *et al.*** *Escherichia coli* toxin/antitoxin pair MqsR/MqsA regulate toxin CspD. *Environ Microbiol* 2010;12:1105–1121.
20. **Wang X, Kim Y, Hong SH, Ma Q, Brown BL *et al.*** Antitoxin MqsA helps mediate the bacterial general stress response. *Nat Chem Biol* 2011;7:359–366.
21. **Hu Y, Benedik MJ, Wood TK.** Antitoxin DinJ influences the general stress response through transcript stabilizer CspE. *Environ Microbiol* 2012;14:669–679.
22. **Huerta-Cepas J, Szklarczyk D, Forslund K, Cook H, Heller D *et al.*** eggNOG 4.5: a hierarchical orthology framework with improved functional annotations for eukaryotic, prokaryotic and viral sequences. *Nucleic Acids Res* 2016;44:D286–D293.
23. **Yang JG, Rees DC.** The allosteric regulatory mechanism of the *Escherichia coli* MetNI methionine ATP binding cassette (ABC) transporter. *J Biol Chem* 2015;290:9135–9140.
24. **Augustus AM, Spicer LD.** The MetJ regulon in gammaproteobacteria determined by comparative genomics methods. *BMC Genomics* 2011;12:558.
25. **Belfaiza J, Guillou Y, Margarita D, Perrin D, Saint Girons I.** Operator-constitutive mutations of the *Escherichia coli* metF gene. *J Bacteriol* 1987;169:670–674.
26. **Gyaneshwar P, Paliy O, McAuliffe J, Jones A, Jordan MI *et al.*** Lessons from *Escherichia coli* genes similarly regulated in response to nitrogen and sulfur limitation. *Proc Natl Acad Sci USA* 2005;102:3453–3458.
27. **Dong T, Yu R, Schellhorn H.** Antagonistic regulation of motility and transcriptome expression by RpoN and RpoS in *Escherichia coli*. *Mol Microbiol* 2011;79:375–386.
28. **Chen Y, Lou S, Fan L, Zhang X, Tan T.** Control of ATP concentration in *Escherichia coli* using synthetic small regulatory RNAs for enhanced S-adenosylmethionine production. *FEMS Microbiol Lett* 2015;362:fnv115.

Edited by: D. Lee and D. Grainger